한국윤활학회지(1992), 제 8권 제 2호
Journal of KSLE(1992) Vol. 8, No. 2, pp.35~43

Propagation Analysis of Surface Crack Due to Hertzian Contact

Seock Sam Kim

Department of Mechanical Engineering, Kyungpook National University, Taegu 702-701, Korea

헤르쯔접촉에 의한 표면균열의 전파해석

김 석 삼

경북대학교 공과대학 기계공학과

요약—취성재료의 마멸천이기구를 규명하기 위해 반무한탄성체상에 표면균열이 존재할 때 그 위를 헤르쯔 접촉하중이 이동할 경우를 해석모델로 하여 선형파괴역학을 도입하여 해석하였다. 해석방법으로는 표면균열을 인상전위의 연속분포로 치환하여 Erdogan-Gupta의 방법으로 균열끝면의 응력확대계수를 구하여, 취성재료의 균열전파조건인 Erdogan-Sih Criterion을 사용하여 그 전파특성을 해석하였다. 본 논문에서는 마멸율이 적은 마멸에서 마멸율이 큰 마멸로 천이할 때 급격한 표면손상과 마찰계수의 급격한 증가를 동반하므로 이에 대한 해석에 중점을 두었다. 해석결과는 접촉하중과 마찰계수의 증가는 표면균열의 전파를 야기시켜 대규모 마멸입자를 생성시키게 됨을 보여주었다.

1. Introduction

Wear process is a removal process of contact area from the operating surface of a body occurring as a result of relative motion at the surface. This removal process is related to deformation and fracture of the contact area. Since the publication of Hornbogen's paper [1] showing the importance of a material's fracture toughness to wear rate, the fracture mechanics approach to the wear mechanism has been attempted. Suh and his co-workers [2-5] attempted to analyze the void nucleation and the driving force for a subsurface crack growth on the basis of fracture mechanics. Rosenfield [6], Hills and Ashelby [7, 8] computed stress intensity factors for subsurface horizontal cracks. Rosenfield emphasized the effects of friction resisting the mode II sliding of crack faces. Keer and his co-workers [9, 10] evaluated the K_I and K_{II} values for both subsurface horizontal cracks and surface breaking vertical cracks without consideration of friction on the crack faces in an elastic half-space loaded by Hertzian contact stresses. More recently, Murakami and his co-workers [11, 12] showed a theoretical demonstration to the mechanism of crack growth from the viewpoint of the fatigue crack propagation in lubricated rolling contact.

However, exact wear mechanisms for the materials have not been clarified. In particular, Hsu and his co-workers [13, 14] reported the wear rates of several ceramics increased suddenly by several orders of magnitude as a result of a slight increase of the test variables. Wear transitions of several ceramics occur as a result of increasing normal contact load, sliding distance or sliding speed. Ceramic materials have been attracted as promising structural materials. From this point of view, it is very important to elucidate the wear mechanisms involved in the transition phenomena of ceramic materials.

The main objective of this paper is to clarify propagation behavior of inclined surface crack under the moving Hertzian contact as the first step to elucidate the wear transition mechanism of ceramic

materials.

In sliding contact, the surface is subjected to a set of normal and tangential stresses which produce deformation and fracture of the materials in a surface layer [15]. The process of fracture consists of plastic flow, formation of microcracks and propagation of these cracks to eventual failure.

2. Method of Analysis

2-1. Statement of the Problem

Consider an elastic half space containing a surface crack inclined at an angle ϕ_0 to the half space surface, as shown schematically in Fig. 1. The surface of the elastic half space is loaded by normal and tangential tractions, defined by eq. (1), which are induced by Hertzian contact sliding that moves along the surface from left to right.

$$P(X_2) = -P_0\sqrt{1-(X_2/C)}, \qquad P_0>0$$
$$Q(X_2) = \mu P(X_2) \tag{1}$$

where P_o is maximum normal Hertzian stress, C half-lengh of Hertzian contact, and μ coefficient of friction at the region of Hertzian contact. In the plane strain condition, the stress component (τ_{xx}, τ_{yy}, τ_{xy}) and displacement gradients ($\partial U_x/\partial x$ and $\partial U_y/\partial x$) can be expressed, in the absence of body force, in terms of the complex potential functions $\Phi(Z)$ and $\Psi(Z)$ [16]:

$$\tau_{xx}+\tau_{yy} = 2[\Phi(Z)+\overline{\Phi(Z)}]$$
$$\tau_{yy}-i\tau_{xy} = \Phi(Z)+\overline{\Phi(Z)}+Z\overline{\Phi'(Z)}+\overline{\Psi(Z)}$$
$$2G\left[\frac{\partial U_x}{\partial x}+i\frac{\partial U_y}{\partial x}\right] = \kappa\Phi(Z)-\overline{\Phi(Z)}-Z\overline{\Phi'(Z)}-\overline{\Psi(Z)} \tag{2}$$

where G is the shear modulus, $Z=x+iy$ and $\kappa=3-4\nu$ for plane strain where ν is Poisson's ratio. The bars imply complex conjugation. Outside of the contact region the surface of the half space is assumed to be free of tractions. Then the boundary conditions specifying normal tractions on the surface of the half space are given as follows:

$$\Phi_2(Z_2)+\overline{\Phi_2(Z_2)}+Z_2\overline{\Phi_2'(Z_2)}+\overline{\Psi_2(Z_2)} = P(X_2)-iQ(X_2) \qquad (Y_2=0,\ |X_2|\le C) \tag{3}$$

$$\Phi_2(Z_2)+\overline{\Phi_2(Z_2)}+Z_2\overline{\Phi_2'(Z_2)}+\overline{\Psi_2(Z_2)} = 0 \qquad (Y_2=0,\ |X_2|\ge C) \tag{4}$$

On the other hand, the requirement that opening region of crack surface be free from tractions and incorporate Coulomb's law of friction in contact region of the crack surface leads to following boundary conditions:

$$\Phi(Z)+\overline{\Phi(Z)}+Z\overline{\Phi'(Z)}+\overline{\Psi(Z)} = 0 \qquad (Y=0,\ 0\le X\le d_0) \tag{5}$$

$$\mathrm{Im}[\Phi(Z)+\overline{\Phi(Z)}+Z\overline{\Phi'(Z)}+\overline{\Psi(Z)}] = \pm\mu'\mathrm{Re}[\Phi(Z)+\overline{\Phi(Z)}+Z\overline{\Phi'(Z)}+\overline{\Psi(Z)}] \qquad (Y=0,\ d_0\le X\le d) \tag{6}$$

where μ' is the coefficient of friction between the contacting crack surfaces, Im and Re mean imaginary part and real part of complex potential functions respectively, the positive sign of μ' corresponds to the case that the upper crack surface slips into the negative x-direction with respect to the lower crack surface, while the negative sign of μ' indicates slipping into the opposite direction. The applied shear stress on the crack surfaces must be greater in magnitude than that of the frictional stress due to the applied normal stress on the crack surfaces. The asymtotic behavior of the complex potential functions at infinity in the half space are:

$$\Phi(Z)=0,\ \Psi(Z)=0 \qquad (|Z|\to\infty) \tag{7}$$

2-2. Singular Integral Equations

The complex potential functions, $\Phi_H(Z_2)$ and $\Psi_H(Z_2)$ [17], which satisfy the boundary conditions (3) and (4) are given by

$$\Phi_H(Z_2) = \frac{P_0(\mu-i)}{2c}(\sqrt{Z_2-c}\,\sqrt{Z_2+c}-Z_2) \tag{8}$$

$$\Psi_H(Z_2) = -\Phi_H(Z_2)-\overline{\Phi_H(Z_2)}-Z_2\Phi'_H(Z_2) \tag{9}$$

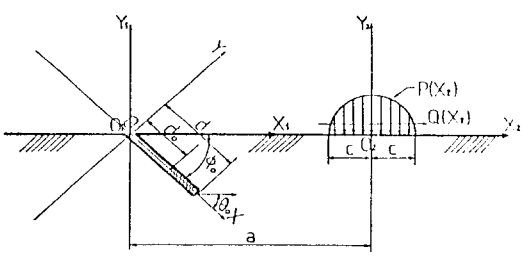

Fig. 1. Analytic model and coordinate systems

where $Z_2=X_2+iY_2$

The complex potential functions $\Phi_H(Z)$ and $\Psi_H(Z)$ referred to the Z-plane are obtained from the $\Phi_H(Z_2)$ and $\Psi_H(Z_2)$ with respect to the Z_2-plane.

In order to apply the method of continuous distributions of dislocations to this crack problem, we derive the complex potential functions $\Phi_D(Z_1)$ and $\Psi_D(Z_1)$ for an isolated edge dislocation, whose slip plane is inclined ϕ from the surface, at a point $Z_1=\alpha$ in Z_1-plane of the semi-infinite medium. Then the complex potential functions are given by [18]

$$\Phi_D(Z_1)=\frac{iGB}{\pi(\kappa+1)}\frac{e^{i\phi}}{Z_1-\alpha}-\frac{iGB}{\pi(\kappa+1)}\left[\frac{e^{i\phi}}{Z_1-\bar{\alpha}}+\frac{(\bar{\alpha}-\alpha)e^{-i\phi}}{(Z_1-\bar{\alpha})^2}\right] \tag{10}$$

$$\Psi_D(Z_1)=-\frac{iGB}{\pi(\kappa+1)}\left[\frac{e^{-i\phi}}{Z_1-\alpha}-\frac{\alpha\, e^{i\phi}}{(Z_1-\alpha)^2}\right]+\frac{iGB}{\pi(\kappa+1)}\left[\frac{e^{-i\phi}}{Z_1-\bar{\alpha}}-\frac{\bar{\alpha}\, e^{i\phi}}{(Z_1-\bar{\alpha})^2}-\frac{(\alpha-\alpha)e^{-i\phi}}{(Z_1-\bar{\alpha})^2}-\frac{2\bar{\alpha}(\bar{\alpha}-\alpha)e^{-i\phi}}{(Z_1-\bar{\alpha})^3}\right] \tag{11}$$

Where B is the Burgers vector of the edge dislocation. It is easily found that the above complex potential functions $\Phi_D(Z_1)$ and $\Psi_D(Z_1)$ satisfy eq. (7). In order to find the complex potential functions satisfying the boundary conditions (5) and (6), the edge dislocations mentioned above will be distributed continuously along the line of the crack. When the edge dislocations whose slip plane is perpendicular to x-axis are distributed at $y=0$ and $0\le x\le d_0$ in the semi-infinite medium, we can obtain the following complex potential functions.

$$\Phi_N(Z)=\frac{G}{\pi(\kappa+1)}\int_0^{d_0}\left[\frac{1}{Z-s}-\frac{e^{i\Phi_0}}{P_1(Z)}+\frac{Q(s)e^{-i\Phi_0}}{P_1^2(Z)}\right]B_1(s)\,ds \tag{12}$$

$$\Psi_N(Z)=\frac{G}{\pi(\kappa+1)}\int_0^{d_0}\left[\frac{1}{Z-s}+\frac{s}{(Z-s)^2}\right]B_1(s)\,ds+\frac{G}{\pi(\kappa+1)}\int_0^{d_0}\left[\frac{-e^{i\Phi_0}}{P_1(Z)}-\frac{s(2e^{i2\Phi_0}-1)}{P_1^2(Z)}+\frac{2sQ(s)}{P_1^3(Z)}\right]B_1(s)\,ds \tag{13}$$

where $P_1(Z)=ze^{i\Phi_0}-se^{-i\Phi_0}$

$Q(s)=s(e^{-i\Phi_0}-e^{i\Phi_0})$

and $B_1(s)$ is dislocation density at a point $z=s$ $(0<s<d_0)$

In the same method, when the edge dislocations whose slip plane is parallel to the x-axis, are distributed at $y=0$ and $0\le x\le d$ in the semi-infinite medium, the complex potential functions are given as follows:

$$\Phi_S(Z)=\frac{iG}{\pi(\kappa+1)}\int_0^{d}\left[\frac{1}{Z-s}-\frac{e^{i\Phi_0}}{P_1(Z)}-\frac{Q(s)e^{-i\Phi_0}}{P_1^2(Z)}\right]B_2(s)\,ds \tag{14}$$

$$\Psi_S(Z)=\frac{iG}{\pi(\kappa+1)}\int_0^{d}\left[-\frac{1}{Z-s}+\frac{s}{(Z-s)^2}\right]B_2(s)\,ds+\frac{iG}{\pi(\kappa+1)}\int_0^{d}\left[\frac{e^{i\Phi_0}}{P_1(Z)}-\frac{s}{P_1^2(Z)}+\frac{2sQ(s)}{P_1^3(Z)}\right]B_2(s)\,ds \tag{15}$$

where $B_2(s)$ is dislocation density at a point $z=s$ $(0<s<d)$. By superposing the solution of above equations, we can obtain the complex potential functions $\Phi(Z)$ and $\Psi(Z)$ which satisfy the boundary conditions (3), (4), and (7).

$$\Phi(Z)=\Phi_H(Z)+\Phi_N(Z)+\Phi_S(Z)$$
$$\Psi(Z)=\Psi_H(Z)+\Psi_N(Z)+\Psi_S(Z) \tag{16}$$

By substituting eq. (16) into eqs. (5) and (6) of the boundary conditions on the crack surface, a system of two coupled singular integral equations for the dislocation density functions $B_1(s)$ and $B_2(s)$ are derived as follows:

$$\int_0^{d_0}\frac{B_1(s)}{X-s}ds+\frac{1}{2}\int_0^{d}k_1(X,s)\,B_1(s)\,ds+\frac{1}{2}\int_0^{d}k_2(X,s)B_2(s)\,ds+\frac{1}{D}Re[F(X)]=0 \tag{17}$$

$$\int_0^{d}\frac{B_2(s)}{X-s}ds+\int_0^{d_0}\left[\frac{1}{2}h_1(X,s)\mp H(X)\mu^c\left[\frac{1}{X-s}+\frac{1}{2}k_1(X,s)\right]\right]B_1(s)\,ds+\frac{1}{2}\int_0^{d}\left[h_2(X,s)\mp H(X)\mu^c k_2(X,s)\right]B_2(s)\,ds+\frac{1}{D}\left[Im[F(X)]\mp H(X)\mu^c Re[F(X)]\right]=0 \tag{18}$$

where $H(X)=\begin{cases}0 & 0\le X\le d_0\\ 1 & d_0\le X\le d\end{cases}$

$$D=\frac{2G}{\pi(\kappa+1)}$$

$$F(X)=\Phi_{oH}(X)+\overline{\Phi_{oH}(X)}+\overline{X\Phi'_{oH}(X)}+\overline{\Psi_{oH}(X)}$$

$$k_1(X,s)+ih_1(X,s)=-\frac{e^{i\phi_0}}{P_1(X)}-\frac{2e^{-i\phi_0}}{\overline{P_1(X)}}+\frac{e^{-i\phi_0}\,Q(s)}{P_1^2(X)}$$
$$+\frac{\overline{Q_1(s)}\,(e^{i\phi_0}+e^{-i\phi_0})}{P_1^2(X)}+\frac{e^{-i2\phi_0}(X-s)}{P_1^2(X)}+\frac{2\overline{Q_1(s)}\,(s-X)}{\overline{P_1^3(X)}}$$

$$k_2(X,s)+ih_2(X,s)=-\frac{ie^{i\phi_0}}{P_1(X)}-\frac{ie^{-i\phi_0}\,Q_1(s)}{P_1^2(X)}$$
$$+\frac{i\overline{Q_1(s)}\,(e^{i\phi_0}+e^{-i\phi_0})}{\overline{P_1^2(X)}}-\frac{ie^{-i2\phi_0}(X-s)}{\overline{P_1^2(X)}}+\frac{i2\overline{Q_1(s)}(s-X)}{\overline{P_1^3(X)}} \tag{19}$$

2-3. Numerical Method of Solution

In order to solve the above simultaneous singular integral eqs. (17) and (18) using the technique developed by Erdogan and Gupta [19, 20], we introduce the following non-dimensional notation:

$$\xi_1=\frac{s}{d_0},\ \eta_1=\frac{x}{d_0},\ \beta_1=\frac{d_o}{c},\ \phi_1(\xi_1)=\frac{\pi D}{P_0}B_1(s)$$
$$\xi_2=\frac{s}{d},\ \eta_2=\frac{x}{d},\ \beta_2=\frac{d}{c},\ \phi_2(\xi_2)=\frac{\pi D}{P_0}B_2(s) \tag{20}$$

$$F(X)=P_0f(\eta_1\beta_1),\quad F(X)=P_0f(\eta_2\beta_2)$$
$$H_o(\eta_2)=\begin{cases}0 & 0\le\eta_2\le d_0/d\\ 1 & d_0/d\le\eta_2\le 1\end{cases}$$

After applying non-dimensional notation terms defined by eq. (20) to eqs (17) and (18), in order to solve numerically the simultaneous singular integral equations by using the method of Erdogan and Gupta [20] we introduce unknown $g_1(\xi_1)$ and $g_2(\xi_2)$ defined by eq. (21).

$$\phi_1(\xi_1)=\frac{g_1(\xi_1)}{\sqrt{1-\xi_1^2}},\ g_1(\xi_1)=g_1(-\xi_1)\ (|\xi_1|<1)$$
$$\phi_2(\xi_2)=\frac{g_2(\xi_2)}{\sqrt{1-\xi_2^2}},\ g_2(\xi_2)=g_2(-\xi_2)\ (|\xi_2|<1) \tag{21}$$

Using the Gauss-Chebyshev integration formula corresponding to the weight function $(1-\xi^2)^{-1/2}$ in the manner developed by Erdogan and Gupta [20] we obtain two systems of linear algebraic equations to determine the unknowns $g_1(\xi_{1k})$ and $g_1(\xi_{2k})$ as follows.

$$\sum_{k=1}^{n}\frac{\pi}{2n+1}\frac{1}{\xi_{1k}-\eta_{1r}}g_1(\xi_{1k})$$
$$-\frac{\beta 1}{2}\sum_{k=1}^{n}\frac{\pi}{2n+1}k_{10}(\eta_{mr},\xi_{nk},\beta_m,\beta_n,\phi_0)\Big|_{\substack{m=1\\n=1}}g_1(\xi_{1k})$$
$$-\frac{\beta 2}{2}\sum_{k=1}^{n}\frac{\pi}{2n+1}k_{20}(\eta_{mr},\xi_{nk},\beta_m,\beta_n,\phi_0)\Big|_{\substack{m=1\\n=2}}g_2(\xi_{2k})$$
$$=\pi\ \mathrm{Re}[f(\eta_{1r},\beta_1)]$$
$$\sum_{k=1}^{n}\frac{\pi}{2n+1}\frac{1}{\xi_{2k}-\eta_{2r}}g_2(\xi_{2k})$$
$$-\sum_{k=1}^{n}\frac{\pi}{2n+1}\Big[\frac{1}{2}h_{10}(\eta_{mr},\xi_{nk},\beta_m,\beta_n,\phi_0)\Big|_{\substack{m=2\\n=1}}\mp H_0(\eta_{2r})\mu^c$$
$$\Big[\frac{1}{\eta_{2r}\beta_2-\xi_{1k}\beta_1}+\frac{1}{2}k_{10}(\eta_{mr},\xi_{nk},\beta_m,\beta_n,\phi_0)\Big|_{\substack{m=2\\n=1}}\Big]\Big]g_1(\xi_{1k})\beta_1$$
$$-\frac{\beta 2}{2}\sum_{k=1}^{n}\frac{\pi}{2n+1}h_{20}(\eta_{mr},\xi_{nk},\beta_m,\beta_n,\phi_0)\Big|_{\substack{m=2\\n=2}}$$
$$\mp H_0(\eta_{2r})\mu^c k_{20}(\eta_{mr},\xi_{nk},\beta_m,\beta_n,\phi_0)\Big|_{\substack{m=2\\n=2}}\Big]\Big]g_2(\xi_{2k})$$
$$=\pi\Big[\mathrm{Im}[f(\eta_{2r},\beta_2)]\mp H_0(\eta_{2r})\mu^c\ \mathrm{Re}[f(\eta_{2r},\beta_2)]\Big] \tag{22}$$

where

$$\eta_{ir}=\cos\Big(\frac{\pi r}{2n+1}\Big),\ r=1,2,\cdots,n$$
$$\xi_{ik}=\cos\Big(\frac{2k-1}{4n+2}\pi\Big),\ r=1,2,\cdots,n$$
$$(i=1,2) \tag{23}$$

In the case of $0<d_0<d$ noting that normal stress at $x=d_0$ has no singularity, we have

$$g_1(1)=0 \tag{24}$$

The stress intensity factors related to the values $g_1(1)$ and $g_2(1)$ at the crack-tip can be expressed as follows:

$$K_I=P_0\sqrt{\pi d}\ g_1(1)$$
$$K_{II}=P_0\sqrt{\pi d}\ g_2(1) \tag{25}$$

2-4. Criteria of Crack Propagation

For pure mode I the crack will propagate in its plane at zero angle from its original direction. For mode II the crack will tend to propagate at approximately 70 degree from its original direction. On the other hand, based on the hypothesis that crack will grow in a direction perpendicular to the maximum tensile stress, Erdogan and Sih [21] proposed the maximum tensile stress criterion for brittle frature in the mixed mode loading. The angle of crack extension, θ_0, is given by one of two roots of the following equation (see Fig. 1).

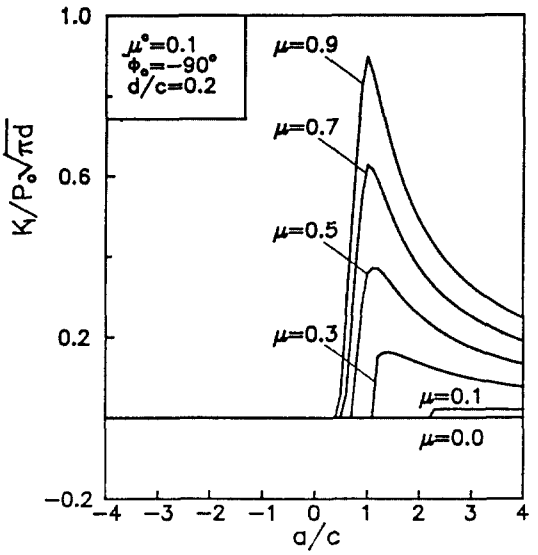

Fig. 2. $K_I/P_0\sqrt{\pi d}$ versus a/c for $\mu^c=0.1$, $\phi_o=-90°$, d/c=0.2, $\mu=0.0$, 0.1, 0.3, 0.5, 0.7, 0.9

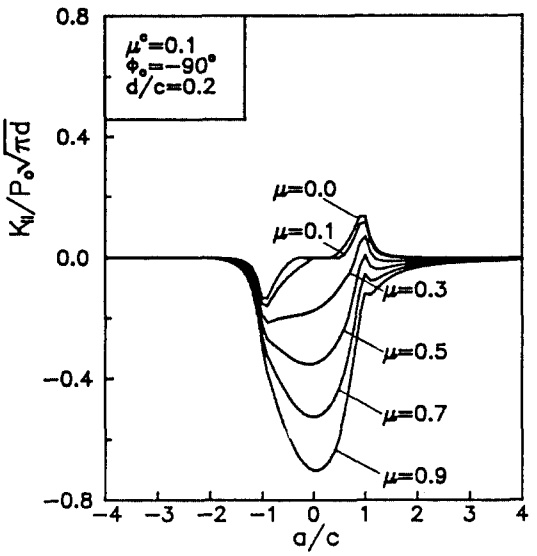

Fig. 3. $K_{II}/P_0\sqrt{\pi d}$ versus a/c for $\mu^c=0.1$, $\phi_o=-90°$, d/c=0.2, $\mu=0.0$, 0.1, 0.3, 0.5, 0.7, 0.9

$$\tan\frac{\theta_0}{2}=\frac{1\pm\sqrt{1+8\gamma^2}}{4\gamma},\quad \gamma=\frac{K_{II}}{K_I} \tag{26}$$

We should choose the angle θ_0 which gives the maximum tangential stress in the polar coordinates (r, θ) defined in Fig. 1.

Because of the obvious nature of the mixed mode loading for the problem, it becomes necessary to consider the effective stress intensity factor that will control the crack propagation. The effective stress intensity factor for the mixed mode which prescribes the distribution of maximum tangential stress at the plane $\theta=\theta_0$ is given by

$$K_{eff}=\cos\frac{\theta_0}{2}\left[K_I\cos^2\frac{\theta_0}{2}-\frac{3}{2}K_{II}\sin\theta_0\right] \tag{27}$$

This theory postulates that if the effective stress intensity factor at the crack-tip equals the critical stress intensity factor K_{IC}, the crack will extend at the crack-tip in the plane normal to the maximum tangential stress.

3. Numerical Results and Discussions

As shown in Fig. 1, we consider the situation that Hertzian contact loading moves along the surface

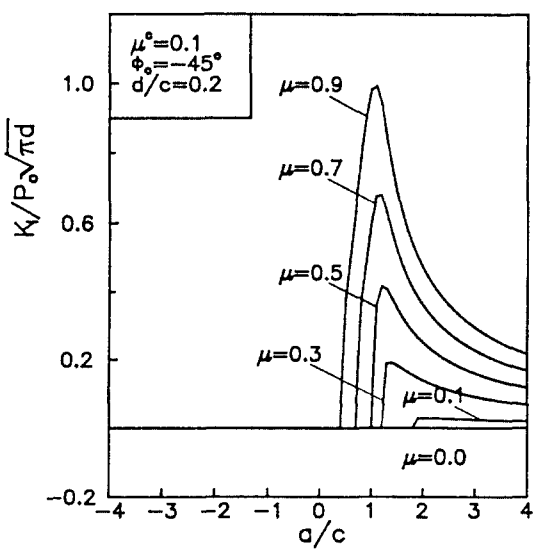

Fig. 4. $K_{eff}/P_0\sqrt{\pi d}$ versus a/c for $\mu^c=0.1$, $\phi_o=-90°$, d/c=0.2, $\mu=0.0$, 0.1, 0.3, 0.5, 0.7, 0.9

of semi-infinite solid containing inclined surface crack from left to right. We investigate the propagation behavior of inclined surface crack on the basis of effective stress intensity factor, K_{eff}, defined by eq. (27). Numerical calculation were performed for the stress intensity factor at the tip of an inclined

surface crack. The variations of dimensionless stress intensity factor, $K_I/P_0\sqrt{\pi d}$, $K_{II}/P_0\sqrt{\pi d}$ and $K_{eff}/P_0\sqrt{\pi d}$ for vertical surface crack ($\phi_0=-90°$) and inclined surface ($\phi_0=-45°$) are shown in Fig. 2~Fig. 9. Figs. 2, 3 and 4 show the numerical results of vertical surface crack for $\mu^c=0.1$, d/c=0.2, and $\mu=0.0$, 0.1, 0.3, 0.5, 0.7 and 0.9. Fig. 2 shows variation of $K_I/P_0\sqrt{\pi d}$ and a/c. As Hertzian contact load moves along the surface of semi-infinite solid from left (a/c=−4) to right (a/c=4) stress field of subsurface varies. Since the stresses in the vicinity of the Hertzian contact are compressive stress which acts to close the crack, so the crack at the position where Hertzian compressive stress applies may be closed. As can be seen from Fig. 2, $K_I/P_0\sqrt{\pi d}$ abruptly increases after a/c=0.4, reach a maximum value at a/c=1.0, and gradually decreases with the movement of Hertzian contact load. Fig. 2 also shows that the magnitude and onset of $K_I/P_0\sqrt{\pi d}$ is directly related to the coefficient of friction of contact surface. $K_I/P_0\sqrt{\pi d}$ increases with the coefficient of friction on the Hertzian contact. Maximum of $K_I/P_0\sqrt{\pi d}$ occurs in the vicinity of trail edge (a/c=1). However, its location is dependent on coefficient of friction. In Fig. 3, $K_{II}/P_0\sqrt{\pi d}$ has alternating shear stress which occurs as the Hertzian contact load passes from left side of the crack to right side of that. Magnitude of $K_{II}/P_0\sqrt{\pi d}$ decreases with coefficient of friction between crack surfaces, μ^c. This result gives us that friction of surface acts as resistance in mode II type crack propagation.

As can be seen from Fig. 3, it is clear that $K_{II}/P_0\sqrt{\pi d}$ is directly related to the coefficient, μ. Fig. 4

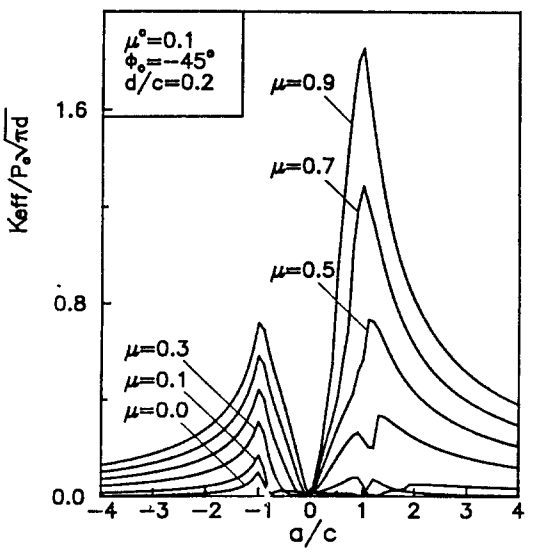

Fig. 6. $K_{II}/P_0\sqrt{\pi d}$ versus a/c for $\mu^c=0.1$, $\phi_o=-45°$, d/c=0.2, μ=0.0, 0.1, 0.3, 0.5, 0.7, 0.9

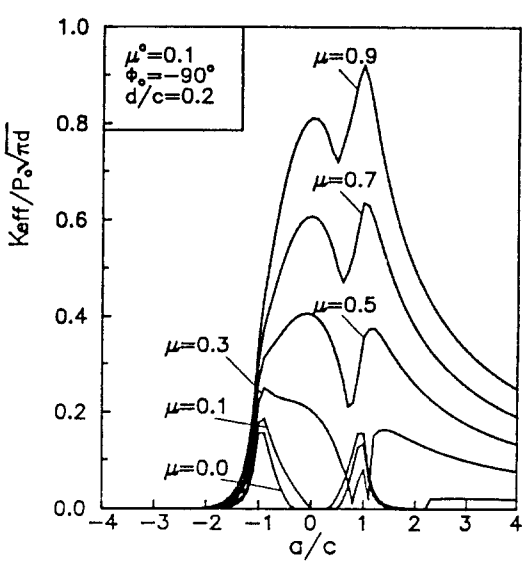

Fig. 5. $K_I/P_0\sqrt{\pi d}$ versus a/c for $\mu^c=0.1$, $\phi_o=-45°$, d/c=0.2, μ=0.0, 0.1, 0.3, 0.5, 0.7, 0.9

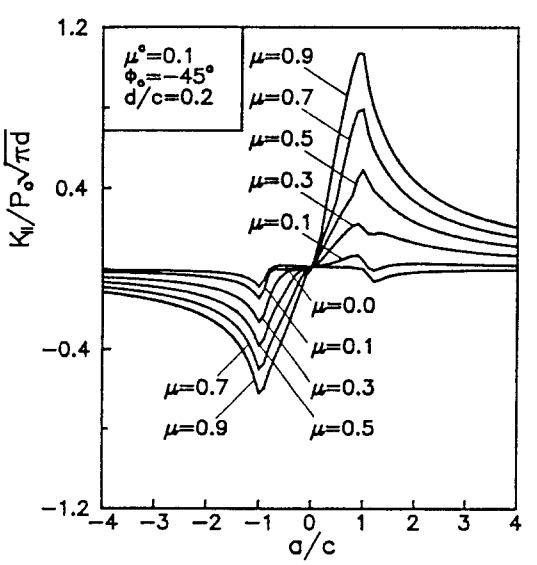

Fig. 7. $K_{eff}/P_0\sqrt{\pi d}$ versus a/c for $\mu^c=0.1$, $\phi_o=-45°$, d/c=0.2, μ=0.0, 0.1, 0.3, 0.5, 0.7, 0.9

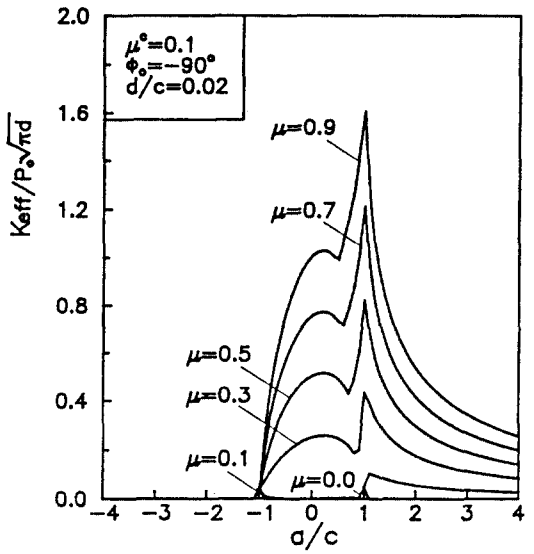

Fig. 8. $K_{eff}/P_0\sqrt{\pi d}$ versus a/c for $\mu^c=0.1$, $\phi_o=-90°$, d/c=0.02, μ=0.0, 0.1, 0.3, 0.5, 0.7, 0.9

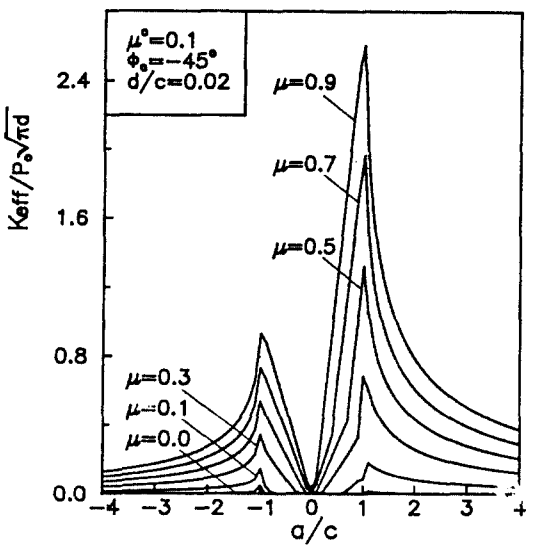

Fig. 9. $K_{eff}/P_0\sqrt{\pi d}$ versus a/c for $\mu^c=0.1$, $\phi_o=-45°$, d/c=0.02, μ=0.0, 0.1, 0.3, 0.5, 0.7, 0.9

indicates variation of dimensionless effective stress intensity factor, $K_{eff}/P_0\sqrt{\pi d}$, when Hertzian contact load moves from left side to right side in the same condition of Figs. 2 and 3. In Fig. 4 it is found that the probability of crack propagation is high at specific point depending on frictional condition. The probability of crack propagation is high at a/c=1.5 and driving force is K_I mode for μ=0.9. On the other hand, the magnitude of $K_{eff}/P_0\sqrt{\pi d}$ resulted from $K_{II}/P_0\sqrt{\pi d}$ is larger than that resulted from $K_I/P_0\sqrt{\pi d}$ in the range of μ<0.5. In general we can define the friction condition by the magnitude of friction coefficient. Accordingly driving force in crack propagation is K_I mode for dry friction (μ>0.7) and K_{II} mode for fluid lubrication (μ<0.1) and boundary lubrication.

Figs. 5 and 6 show the variation of $K_I/P_0\sqrt{\pi d}$ and $K_{II}/P_0\sqrt{\pi d}$ in the case of $\mu^c=0.1$, boundary lubrication of crack surfaces, for $\phi_0=-45°$ and d/c=0.2, and μ=0.0, 0.1, 0.3, 0.5, 0.7 and 0.9. Fig. 7 shows also the variation of dimensionless effective stress intensity factor, $K_{eff}/P_0\sqrt{\pi d}$, for the same condition of Figs. 5 and 6. From Figs. 2 and 5, $K_I/P_0\sqrt{\pi d}$ has almost same tendency. However, Figs 3 and 6 show that $K_{II}/P_0\sqrt{\pi d}$ has different tendency because of much complicated stress field below the Hertzian contact. Fig. 6 indicates that magnitude of $K_{II}/P_0\sqrt{\pi d}$ is related to the coefficient of friction on Hertzian contact. Fig. 7 shows that inclined crack has higher probability of mode II crack propagation than mode I crack propagation in comparison with same crack length of vertical crack.

Figs. 8 and 9 are results of d/c=0.02, for $\mu^c=0.1$, boundary lubrication, vertical and inclined crack, respectively. Figures show the variation of dimensionless effective stress intensity factor, $K_{eff}/P_0\sqrt{\pi d}$. As can be seen from these figures, coefficient of friction is very important for crack propagation. The increase in the level of surface damage seems to correlate with the coefficient of friction. Severe wear is, in most cases, caused by surface damage. The rise of the coefficient of friction at the wear transition point implies the larger surface roughness developed by wear. It is confirmed that crack propagation from pre-existing cracks controls the wear transition. In this respect, reduction of the coefficient of friction or the contact stress can prevent the wear transition. The coefficient of friction can be reduced by lubrication (both liquid and solid) and/or by the formation of tribochemical films. Investigators confirmed the formation of tribochemical films on ceramic surfaces in sliding contact

[22-25].

4. Conclusions

Based on linear fracture mechanics, theoretical analysis was conducted on the propagation characteristics of an inclined surface crack under the plane strain condition subjected to Hertzian contact loading. In particular, this paper investigated the effects of friction of Hertzian contact and between surface crack faces, the effects of crack length and crack inclination. Analytic results have shown that driving force for crack propagation is K_{II} mode for fluid and boundary friction. The coefficient of friction at the Hertzian contact and crack surfaces plays an important role in the wear transition. The wear transition can be prevented by the reduction of the contact stress or the coefficient of friction, and by the formation of tribochemical films.

Acknowledgements

The author is grateful for the financial support received from the Post-Doc. Program of Korea Science and Engineering Foundation. The author also thanks Dr. S.M. Hsu of NIST for his discussions.

Nomenclature

a	: distance from origin to contact centerline
B	: dislocation density
c	: half length of Hertzian contact
d	: crack length
d_0	: length of opening crack part
G	: shear modulus
K_I, K_{II}	: stress intensity factors
K_{eff}	: effective stress intensity factor
P_0	: maximum Hertzian contact stress
ϕ_0	: crack inclination angle (degree)
Φ, Ψ	: complex potential function
ν	: Poisson ratio
μ, μ'	: coefficient of friction for Hertzian contact and crackfaces
θ_0	: angle from crackline of maximal stress for crack extention

References

1. Hornbogen, E., "The Role of Fracture Toughness in the Wear of Metals", Wear, Vol. 33, 1975, pp. 251-259.
2. Suh, N.P., "An Overview of the delamination Theory of Wear", Wear, Vol. 44, 1977, pp. 1-16.
3. Jahanmir, S. and Suh, N.P., "Mechanics of Subsurface Void Nucleation in Delamination Wear", Wear, Vol. 44, 1977, pp. 17-38.
4. Fleming, J.R. and Suh, N.P., "Mechanics of Crack Propagation in Delamination Wear", Wear, Vol. 44, 1977, pp. 39-56.
5. Fleming, J.R. and Suh, N.P., "The Relationship Between Crack Propagation Rates and Wear Rates", Wear, Vol. 44, 1977, pp. 57-64.
6. Rosenfield, A.R., "A Fracture Mechanics Approach to Wear", Wear, Vol. 61, 1980, pp. 125-132.
7. Hills, D.A. and Ashelby, D.W., "On the Determination of Stress Intensification Factors for a Wearing Half-Space", *Eng. Fract. Mech.* Vol. 13, 1980. pp. 69-78.
8. Hills, D.A. and Ashelby, D.W., "On the Application of Fracture Mechanics to Wear", Wear, Vol. 54, 1980, pp. 321-330.
9. Keer, L.M., Bryant, M.D. and Haritos, G.K., "Subsurface and surface Cracking Due to Hertzian Contact", ASME Journal of Lubrication Technology, Vol. 104, 1982, pp. 347-351.
10. Keer, L.M. and Bryant, M.D., "A Pitting Model for Rolling Contact Fatigue", ASME Journal of Lubrication Technology, Vol. 105, 1983, pp. 198-205.
11. Murakami, Y., Kaneta, M. and Yatsuzuka, H., "Analysis of Surface Crack Propagation in Lubricated Rolling Contact", *ASLE Trans.*, Vol. 28, 1985, pp. 60-68.
12. Kaneta, M., Yatsuzuka, H. and Murakami, Y., "Mechanism of Crack Growth in Lubricated Rolling/Sliding Contact", *ASLE Trans.*, Vol. 28, 1985, pp. 407-414.
13. Hsu, S.M., Wang, Y.S. and Munro, R.G., "Quantitative Wear Maps as a Visualization of Wear Mechanism Transitions in Ceramic Materials", Wear of Materials, Vol. 2, K.C. Ludema (Ed.), American Society of Mechnical Engineers, New York, NY, 1989, pp. 723-728.
14. Deckman, D.E., Jahanmir, S., Hsu, S.M. and Gates, R.S., "Friction and Wear Measurements for New Materials and Lubricants", Engineered Materials for Advanced Friction and Wear Applications, F.A. Smidt andd P.J. Blau (Eds), ASM International, Matals Park, OH, 1988, pp. 167-168.
15. Jahanmir, S., "On Mechanics and Mechanisms of Laminar Wear Particle Formation", Advances in the Mechanics and Physics of Surfaces, Vol. 3, R.M.

Latanision and T.E. Fischer (Eds.), Harwood Academic, New York, NY, 1986, pp. 261-331.
16. Muskhelishvili, N.I., "Some Basic Problems of the Mathematical Theory of Elasticity, Noordhoff, The Netherlands, 1963.
17. Kim, S.S., Abe, H., Hayashi, K., Kato, K. and Hokkirigawa, K., "Analysis of Rolling Wear Mechanism of Ceramics Based on Fracture Mechanics-Part 2", *Proc. 32nd JSLE conf.*, 1988, pp. 289-292.
18. Tamate, O., Deformation of Elastic Solid, Corona, Tokyo, 1971, pp. 209-265.
19. Erdogan, F. and Gupta, G.D., "On the Numerical Solution of Singular Integral Equations", Quarterly of Applied Mathematics, Vol. 32, 1972, pp. 525-534.
20. Gupta, G.D. and Erdogan, F., "The Problem of Edge Cracks in an Infinite Strip", *ASME Journal of Applied Mechanics*, Vol. 41, 1974, pp. 1001-1006.
21. Erdogan, F. and Sih, G.C., "On the Crack Extension in Plates Under Plane Loading and Transverse Shear", *ASME Journal of Basic Engineering*, Vol. 85, 1963, pp. 519-527.
22. Tomizawa, H. and Fischer, T.E., "Friction and Wear of Silicon Nitride at 150℃ to 800℃", *ASLE Trans.*, Vol. 29, 1986, pp. 481-488.
23. Fischer, T.E. and Tomizawa, H., "Interaction of Tribochemistry and Microfracture in the Friction and Wear of Silicon Nitride", Wear, Vol. 105, 1985, pp. 29-45.
24. Jahanmir, S. and Fischer, T.E., "Friction and Wear of Silicon Nitride Lubricated by Humid Air, Water, Hexadecane and Hexadecane+0.5 Percent Stearic Acid", *Tribology Transactions*, Vol. 31, 1988, pp. 32-43.
25. Gates, R.S., Hsu, S.M. and Klaus, E.E., "Tribochemical Mechanism of Alumina with Water", *Tribology Transactions*, Vol. 32, 1989, pp. 357-363.